Since January 2020 Elsevier has created a COVID-19 resource centre with free information in English and Mandarin on the novel coronavirus COVID-19. The COVID-19 resource centre is hosted on Elsevier Connect, the company's public news and information website.

Science of the Total Environment 813 (2022) 152345

Contents lists available at ScienceDirect

Science of the Total Environment

journal homepage: www.elsevier.com/locate/scitotenv

Toxicity of spike fragments SARS-CoV-2 S protein for zebrafish: A tool to study its hazardous for human health?

Bianca H. Ventura Fernandes [a], Natália Martins Feitosa [b], Ana Paula Barbosa [c], Camila Gasque Bomfim [c], Anali M.B. Garnique [d], Ivana F. Rosa [e], Maira S. Rodrigues [e], Lucas B. Doretto [e], Daniel F. Costa [e], Bruno Camargo-dos-Santos [f], Gabrielli A. Franco [f], João Favero Neto [f], Juliana Sartori Lunardi [f], Marina Sanson Bellot [f], Nina Pacheco Capelini Alves [f], Camila C. Costa [g], Mayumi F. Aracati [g], Letícia F. Rodrigues [g], Camila C. Costa [g], Rafaela Hemily Cirilo [f], Raul Marcelino Colagrande [f], Francisco I.F. Gomes [h], Rafael T. Nakajima [e], Marco A.A. Belo [i], Percília Cardoso Giaquinto [j], Susana Luporini de Oliveira [k], Silas Fernandes Eto [l], Dayanne Carla Fernandes [m], Wilson G. Manrique [n], Gabriel Conde [o], Roberta R.C. Rosales [p], Iris Todeschini [q], Ilo Rivero [r], Edgar Llontop [q], Germán G. Sgro [q,s], Gabriel Umaji Oka [q], Natalia Fernanda Bueno [q], Fausto K. Ferraris [t], Mariana T.Q. de Magalhães [u], Renata J. Medeiros [v], Juliana M. Mendonça-Gomes [w], Mara Souza Junqueira [x], Kátia Conceição [y], Leticia Gomes de Pontes [z], Antonio Condino-Neto [z], Andrea C. Perez [ab], Leonardo J.G. Barcellos [ab,ac], José Dias Correa Júnior [ad,ae], Erick Gustavo Dorlass [af], Niels O.S. Camara [w], Edison Luiz Durigon [c], Fernando Q. Cunha [ag], Rafael H. Nóbrega [e], Glaucia M. Machado-Santelli [ah], Chuck S. Farah [q], Flavio P. Veras [ai,aj], Jorge Galindo-Villegas [ak], Letícia V. Costa-Lotufo [al], Thiago M. Cunha [ai,aj], Roger Chammas [am], Luciani R. Carvalho [an], Cristiane R. Guzzo [c], Guilherme Malafaia [ao,*], Ives Charlie-Silva [al,**]

[a] Laboratório de Controle Genético e Sanitário, Diretoria Técnica de Apoio ao Ensino e Pesquisa, Faculdade de Medicina da Universidade de São Paulo, Brazil
[b] Laboratório Integrado de Biociências Translacionais (LIBT), Instituto de Biodiversidade e Sustentabilidade (NUPEM), Universidade Federal do Rio de Janeiro (UFRJ), Macaé, RJ, Brazil
[c] Department of Microbiology, Institute of Biomedical Sciences, University of Sao Paulo, Sao Paulo, Brazil
[d] Department of Cell Biology, Institute of Biomedical Sciences, University of São Paulo, Brazil
[e] Reproductive and Molecular Biology Group, Department of Morphology, Institute of Biosciences, Sao Paulo State University, Botucatu, São Paulo, Brazil
[f] Department of Structural and Functional Biology, Institute of Biosciences of Botucatu, São Paulo State University, SP, Brazil
[g] Department of Preventive Veterinary Medicine, São Paulo State University (UNESP), Jaboticabal, Brazil
[h] Department of Pharmacology, Center of Research in Inflammatory Diseases, Ribeirao Preto Medical School, University of São Paulo, Brazil
[i] Brasil University, Descalvado, São Paulo, Brazil
[j] Universidade Estadual Paulista Júlio de Mesquita Filho, Instituto de Biociências - Departamento de Fisiologia, São Paulo, Brazil
[k] Universidade Estadual Paulista Júlio de Mesquita Filho, São Paulo, Brazil
[l] Postgraduate Program in Health Sciences, PROCISA, Federal University of Roraima, Brazil
[m] Immunochemistry Laboratory, Butantan Institute, São Paulo, Brazil
[n] Aquaculture Health Research and Extension Group, GRUPESA, Aquaculture Health Laboratory, LABSA, Department of Veterinary Medicine, Federal University of Rondônia, Rolim de Moura campus, Rondônia, Brazil
[o] Department of Preventive Veterinary Medicine, São Paulo State University, Jaboticabal, Brazil
[p] Department of Cell and Molecular Biology, Ribeirao Preto Medical School, University of São Paulo, Ribeirão Preto, Brazil
[q] Departamento de Bioquímica, Instituto de Química, Universidade de São Paulo, Brazil
[r] Pontifícia Universidade Católica de Minas Gerais, Brazil
[s] Departamento de Ciências Biomoleculares, Faculdade de Ciências Farmacêuticas de Ribeirão Preto, Universidade de São Paulo, Ribeirão Preto, SP, Brazil
[t] Department of Pharmacology and Toxicology, Oswaldo Cruz Foundation, FIOCRUZ, Rio de Janeiro, Brazil
[u] Department of Biochemistry and Immunology, Institute of Biological Sciences, Federal University of Minas Gerais, Belo Horizonte, Brazil
[v] Laboratory of Physiology, INCQS/Fiocruz Zebrafish Facility, Departament of Pharmacology and Toxicology, National Institute for Quality Control in Health, Brasil
[w] Transplantation Immunobiology Lab, Department of Immunology, Institute of Biomedical Sciences, Universidade de Sao Paulo, Brazil
[x] Center for Translational Research in Oncology, Cancer Institute of the State of Sao Paulo, Faculty of Medicine, University of São Paulo, Sao Paulo, Brazil
[y] Laboratory of Peptide Biochemistry, Federal University of São Paulo, Brazil
[z] Laboratory of Human Immunology, Department Immunology, Institute Biomedical Sciences, University São Paulo, Sao Paulo, Brazil
[aa] Department of Pharmacology, Universidade Federal de Minas Gerais, Brazil
[ab] Graduate Program of Pharmacology, Federal University of Santa Maria, Brazil
[ac] Laboratory of Fish Physiology, Graduate Program of Bioexperimentation and of Environmental Sciences, University of Passo Fundo, Brazil

* Correspondence to: G. Malafaia, Biological Research Laboratory, Goiano Federal Institution – Urata Campus, Rodovia Geraldo Silva Nascimento, 2,5 km, Zona Rural, Urutaí, Brazil.
** Corresponding author.
E-mail addresses: guilhermeifgoiano@gmail.com (G. Malafaia), charliesilva4@hotmail.com (I. Charlie-Silva).

http://dx.doi.org/10.1016/j.scitotenv.2021.152345

[ad] Laboratório do Estudo da Interação Químico Biológica e da Reprodução Animal, LIQBRA, Bloco O3,174, Brazil
[ae] Departamento de Morfologia Instituto de Ciências Biológicas, Universidade Federal de Minas Gerais, Brazil
[af] Department of Microbiology, Institute of Biomedical Sciences, University of Sao Paulo, Brazil
[ag] Department of Pharmacology, Center of Research in Inflammatory Diseases, Ribeirao Preto Medical School, University of São Paulo, Ribeirão Preto, Brazil
[ah] Department of Cell Biology, Institute of Biomedical Sciences, University of São Paulo, São Paulo, Brazil
[ai] Center of Research in Inflammatory Diseases, Ribeirão Preto Medical School, University of Sao Paulo, Ribeirão Preto, Sao Paulo, Brazil
[aj] Department of Pharmacology, Ribeirao Preto Medical School, University of São Paulo, Ribeirao Preto, São Paulo, Brazil
[ak] Faculty of Biosciences and Aquaculture, Nord University, 8049 Bodo, Norway
[al] Department of Pharmacology, Institute of Biomedical Sciences, Universidade de São Paulo, Brazil
[am] Centro de Investigação Translacional em Oncologia, Instituto do Câncer do Estado de São Paulo, Faculdade de Medicina da Universidade de São Paulo, Brazil
[an] Disciplina de Endocrinologia do Departamento de Clinica Medica e Laboratório de Hormônios e Genética Molecular, LIM 42, Brazil
[ao] Biological Research Laboratory, Goiano Federal Institute, Urutaí Campus, Brazil

HIGHLIGHTS

- Use of *Danio rerio* a in favor of the conservation of non-target species against SARS-CoV-2
- Zebrafish as a tool to assess the harmful effects of SARS-CoV-2 in the aquatic environment
- Zebrafish injected with SARS-CoV-2 rSpike protein shows several morphological alterations.
- In silico studies have shown interactions between rSpike protein and ACE2.
- Role of ACE2 gene expression in all the system in Zebrafish shows like human.

GRAPHICAL ABSTRACT

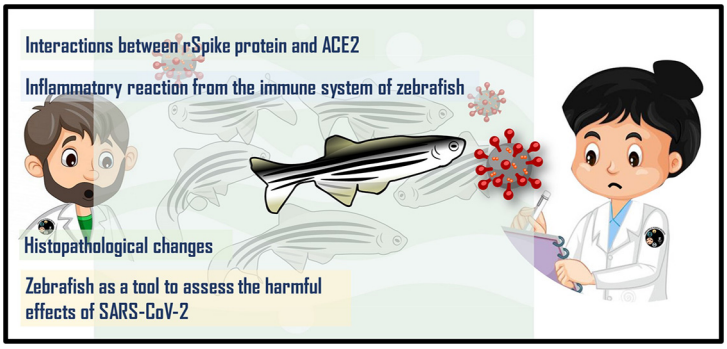

ARTICLE INFO

Article history:
Received 30 September 2021
Received in revised form 17 November 2021
Accepted 8 December 2021
Available online 21 December 2021

Keywords:
Coronavirus
Danio rerio
Environmental impacts
Infection diseases
Acute respiratory syndrome

ABSTRACT

Despite the significant increase in the generation of SARS-CoV-2 contaminated domestic and hospital wastewater, little is known about the ecotoxicological effects of the virus or its structural components in freshwater vertebrates. In this context, this study evaluated the deleterious effects caused by SARS-CoV-2 Spike protein on the health of *Danio rerio*, zebrafish. We demonstrated, for the first time, that zebrafish injected with fragment 16 to 165 (rSpike), which corresponds to the N-terminal portion of the protein, presented mortalities and adverse effects on liver, kidney, ovary and brain tissues. The conserved genetic homology between zebrafish and humans might be one of the reasons for the intense toxic effects followed inflammatory reaction from the immune system of zebrafish to rSpike which provoked damage to organs in a similar pattern as happen in severe cases of COVID-19 in humans, and, resulted in 78,6% of survival rate in female adults during the first seven days. The application of spike protein in zebrafish was highly toxic that is suitable for future studies to gather valuable information about ecotoxicological impacts, as well as vaccine responses and therapeutic approaches in human medicine. Therefore, besides representing an important tool to assess the harmful effects of SARS-CoV-2 in the aquatic environment, we present the zebrafish as an animal model for translational COVID-19 research.

1. Introduction

COVID-19 (Coronavirus Disease-2019), caused by SARS-CoV-2 (Severe Acute Respiratory Syndrome Coronavirus 2) has had unprecedented global impacts. Economically, the exact magnitude of the losses is still uncertain, but the short and long-term fiscal and budgetary effects indicate that we are heading for the biggest recession in contemporary history (McKibbin and Fernando, 2020). Socially, the disease has strongly influenced the daily lives of millions of people, from the obligation to follow rules of social isolation, with the simultaneous closure of borders imposed by the governments of some countries, to the planning and adoption of health measures to face a still incipient crisis. According to the World Health Organization (WHO), the most recent estimates on the status of the pandemic in the world record more than 246,592,349 million confirmed cases and more than 5,001,138 million deaths worldwide in November 2021 (World Health Organization (WHO), n.d.).

As far as we know, the classic form of transmission of SARS-CoV-2 is by air and via contact with infected people (Harrison et al., 2020; Meyerowitz et al., 2021). Nonetheless, several forms of transmission of the new coronavirus have been investigated, motivated by the persistence of the virus in the environment for a few hours/days. According to Kampf et al. (2020), the virus can survive on inanimate surfaces such as metal, glass, or plastic for up to 9 days if no disinfection procedure (e.g.: 62–71% ethanol, 0.5% hydrogen peroxide or 0.1% sodium hypochlorite within 1 min) is performed. Another form of transmission is the excrement of infected people, since many studies have shown the presence of SARS-CoV-2 viral titers in domestic sewage (Elsamadony et al., 2021; Moghadas et al., 2020), especially from human urine and feces (Jones et al., 2020; Sun et al., 2020; Xiao et al., 2020). Longitudinal analysis of wastewater can be used to identify trends in disease transmission before reporting clinical cases and can shed light on characteristics of infection that are difficult to capture in clinical investigations, such as the dynamics of early viral elimination (Adhikari et al., 2020). In this scenario, as discussed by Liu et al. (2020), the potential for secondary transmission of the SARS-CoV-2 virus via wastewater should not be underestimated (Teymoorian et al., 2021).

The SARS-CoV-2 Spike (S) protein is found on the surface of the SARS-CoV-2 virus, giving it a "crown" appearance (Coughlan, 2020). This protein plays a key role in the infection process, triggering the fusion process in the cell membrane (Lan et al., 2020). The trimeric spike protein belongs to the class I fusion proteins. Its two subunits S1 and S2 orchestrate its entrance into the cell, while S1 subunit facilitates the attachment of the virus via its receptor-binding domain (RBD) to the host cell receptor (angiotensin

converting enzyme 2) (ACE2), the S2 subunit mediates the fusion of the viral and human cellular membranes (Hoffmann et al., 2020; Shang et al., 2020; Zamorano Cuervo and Grandvaux, 2020). In addition, Spike protein has been considered one of the potential candidates as an antigen for the production of vaccines against COVID-19 (Bangaru et al., 2020; Fan et al., 2020; Keech et al., 2020; Ravichandran et al., 2020; Samrat et al., 2020; Wang et al., 2020a).

On the other hand, a field still little explored refers to the possible environmental impacts (direct and indirect) of the current outbreak of COVID-19. Despite the increase in contaminated household (Gautam and Sharma, 2020; Urban and Nakada, 2021; Zand and Heir, 2020) and hospital (Abu-Qdais et al., 2020; Sangkham, 2020; Wang et al., 2020b) waste generation, so far, there is no information on the ecotoxicological effects of SARS-CoV-2 or its structural components on freshwater vertebrates. Therefore, these facts justify the urgent need for studies in order to assess the deleterious effects caused by SARS-CoV-2 virus on the health of aquatic organisms which already suffer as a result of various anthropic activities. In addition to its significant importance in public health, such studies might support actions or strategies to mitigate these impacts in favor of the conservation of non-target species.

2. Material and methods

2.1. Production of recombinant spike protein SARS-CoV-2

Cloning, expression, and protein purification. The DNA fragment coding for the SARS-CoV-2 Spike protein fragment from 16 to 165 (rSpike) was amplified by PCR using SARS-CoV-2 cDNA transcribed from the RNA isolated from the second patient, strain HIAE-02:SARS-CoV-2/SP02/human/2020/BRA (GenBank accession number MT126808.1). The primers used for amplification of the Spike fragment are 5′ AGCATAGCTAGCGTTAATC TTACAACCAGAACTCAATTACC 3′ and 5′ ATTATCGGATCCTTAATTATT CGCACTAGAATAAACTCTGAAC 3′. The PCR product was purified using the GeneJET PCR Purification Kit (Thermo Fisher Scientific, ref. #K0702) and digested with AnzaTM restriction enzymes *Nhe*I and *BamH*I (Thermo Fisher Scientific). The expression vector used was pET-28a that was also digested with the same pair of restriction enzymes as the amplified rSpike DNA fragment. The digested fragment was used to ligate the rSpike DNA fragment to the digested pET-28a vector using T4 DNA ligase (Thermo Fisher Scientific). The positive clones were confirmed by digestion tests. The rSpike cloned into pET28a results in a protein with a fusion of seven histidine tag at the N-terminal portion of the protein to facilitate the protein purification steps.

rSpike was expressed in *Escherichia coli* strain BL21(DE3) and BL21 (DE3) Star. The cells were grown in 2XTY medium (16 g/L of bactotryptone, 10 g/L of yeast extract, and 5 g/L sodium chloride) with added kanamycin (50 μg/ml) under agitation at 37 °C to an OD_{600nm} of 0.6, at which point 0.5 mM isopropyl-β-D-1-thiogalactopyranoside (IPTG) was added. After 4 h of induction, the cells were collected by centrifugation (4500 ×*g*, 4 °C, 15 min) and stored at −80 °C. The cell pellet expressing the rSpike protein was resuspended in lysis buffer [50 mM 3-(*N*-morpholino)propanesulfonic acid (MOPS) pH 7.0, 200 mM NaCl, 5% glycerol, 0.03% Triton-100 and 0.03% Tween-20] and lysed by sonication on an ice bath in a Vibracell VCX750 Ultrasonic Cell Disrupter (Sonics, Newtown, CT, USA). The lysate was centrifuged at 30,000 ×*g*, 4 °C for 45 min. The pellet fraction was resuspended in 7 M urea, 50 mM MOPS pH 7.0, 200 mM NaCl, and 20 mM imidazole on an ice bath under agitation for 1 h and centrifuged at 30,000 ×*g*, 4 °C for 45 min. The soluble fraction was loaded in a HisTrap Chelating HP column (GE Healthcare Life Sciences) previously equilibrated with 7 M urea, 50 mM MOPS pH 7.0, 200 mM NaCl, and 20 mM imidazole. Bound proteins were eluted using a linear gradient of imidazole over 20 column volumes (from 20 mM to 1 M imidazole). Fractions with rSpike were concentrated using Amicon Ultra-15 Centrifugal filters (Merck Millipore) with a 3 kDa membrane cutoff and loaded onto a HiLoad 16/600 Superdex 75 pg (GE Healthcare Life Sciences) size exclusion chromatography column previously equilibrated with 7 M urea, 50 mM MOPS pH 7.0, 200 mM NaCl, and 1 mM EDTA. The eluted fractions were analyzed by 15% SDS-PAGE for purity, and the fractions containing the target protein were mixed and concentrated using Amicon Ultra-15 Centrifugal filters (Merck Millipore) with a 3 kDa membrane cutoff (Fig. 1b).

2.2. Zebrafish maintenance

Wild-type zebrafish from the AB line, and specific pathogen-free (SPF), were raised in Tecniplast Zebtec (Buguggiate, Italy) and maintained in the zebrafish housing systems in the Faculty of Medicine of the University of São Paulo facilitie, SP. Brazil. Fish used for the experiments were obtained from natural crossings and raised according to standard methods (Tsang et al., 2017). Zebrafish were kept in 3.5 L polycarbonate tanks and fed three times a day with Gemma micro by Skretting (Stavanger, Norway). The photoperiod was 14:10 h light-dark cycle and the water quality parameters were 28 °C ± ,05 °C; pH = 7.3 ± 0.2; conductivity 500 to 800 μS/cm, referred to as system water. The procedures were approved by the Ethics Committee (CEUA) of the Faculty of Medicine of the University of São Paulo and registered under protocol number 1514/2020.

2.3. The administration spike in adult zebrafish

We performed 2 intraperitoneal (IP) inoculations of a solution containing 1 μg purified rSpike diluted in 10 μL of inoculation buffer (7 M urea, 50 mM Tris-HCl pH 7.5, 200 mM NaCl, and 1 mM EDTA). A group of control animals received injections containing only the dilution buffer. Another control group was challenged by a lysate of bacterial fragment of *E. coli* BL21(DE3) extract. rSpike was injected into two injected sections in 20 zebrafish females (previously anesthetized with tricaine methanesulfonate (Sigma) - at a concentration of 150 mg/L) at an interval of 7 days, with the aim of producing plasma antibodies. Passive antibody transfer to zebrafish eggs occurs naturally as described by Wang et al. (2020b). After injected, females were stimulated to mate (at 7 and 14 days after injection) and generated eggs. The time at which the antibodies were transferred to the eggs was analyzed by the western blot technique. Another control group was performed using 1 μg of a mix of proteins in buffer 50 mM Tris-HCl pH 8.0, 200 mM NaCl, and 1 mM EDTA: equivalent amount of purified PilZ protein from *Xanthomonas citri pv. citri.* (Guzzo et al., 2009) and LIC_11128 (residues 1–115 cloned into pET28a expression vector a with a fusion of seven histidine tag at the N-terminal portion of the protein) from *Leptospira interrogans*.

2.4. Histology from multiple organs

For histopathological analysis, 5 fishes from control, 5 from naïve and 20 injected with rSpike were fixed in 10% formaldehyde for 24 h and then dehydrated in ethanol, embedded in paraffin, and sectioned (5 μm). The sections were stained with hematoxylin and eosin and analyzed under an optical microscope. This methodology was adapted from described by Luna and Moore et al. (2002). The heart, kidney, liver, spleen, ovary, brain, intestine, eye, mesentery, Langerhans islands, muscular tissue and gills were qualitatively evaluated considering presence or absence of structural alterations. The slides were analyzed and photographed using a 10, 20 and 40-times objective Olympus model B × 51 (Olympus Corporation) microscope coupled to a 2-times projected Q Color 3 Olympus model U-PMTVC (Olympus Corporation). The pro-gram used for photographic records was the QCapture (Q Imaging) image analysis program. Then, the images obtained were treated for adjustment of size, contrast, brightness, and focus, as well as mounted on planks and subtitled using the program Adobe Photoshop CC 2017. Histopathological analysis of different organs, including brain, gonads, heart, kidney, liver, spleen, among others, was performed in female fishes used in the injected protocol described in material and methods. The occurrence or absence of pathological characteristic was used as qualitative criteria for the organs analyzed and grouped

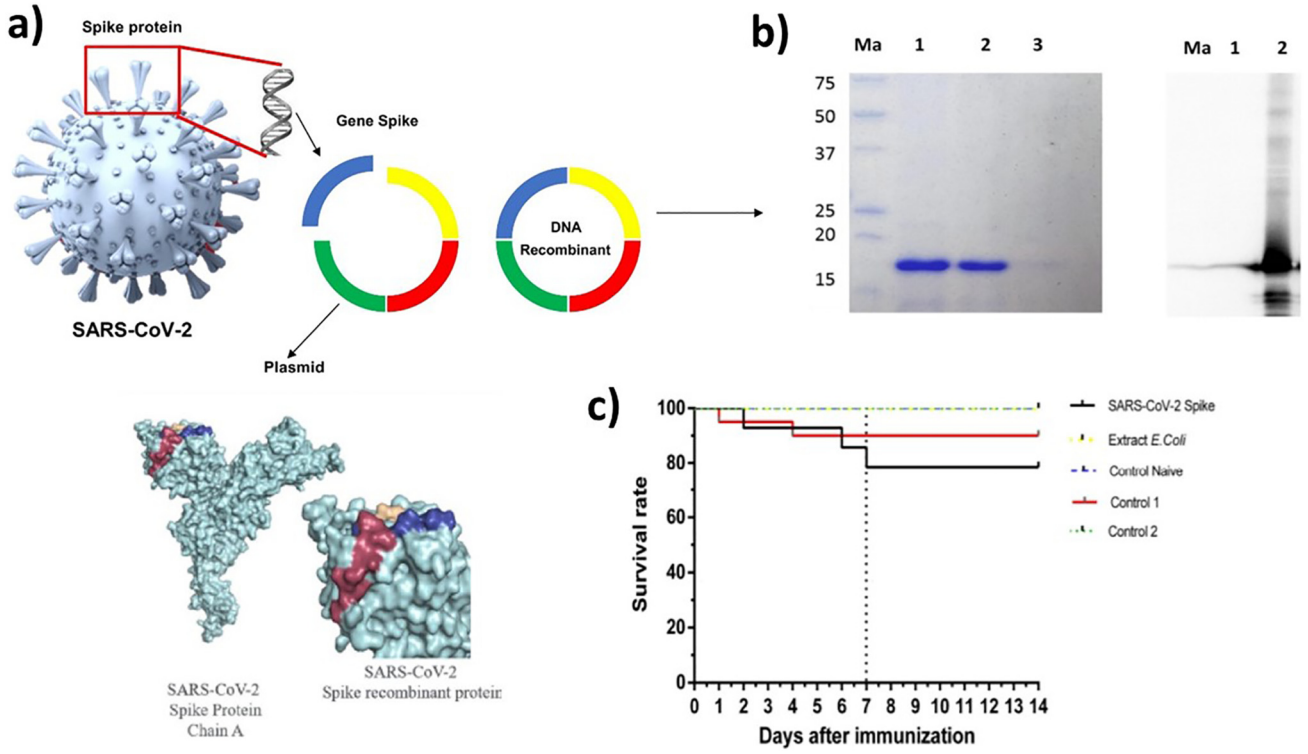

Fig. 1. (A) protein expression of SARS-CoV-2 spike protein fragment. For this, the DNA fragment coding for spike of the SARS-CoV-2 full-length S protein; (B) purified spike protein samples tested in SDS-PAGE gel with Coomassie Blue stain, end for purity; Anti-HisTag Western Blot reactivity, for specificity; (C) rSpike protein injection is toxic to adult female zebrafish. Graph of survival rate and days after injected. Kaplan-Meier cumulative probability curve indicating survival rate of zebrafish after two injected with different protein samples. Females were injected either with rSpike protein, extract of lysed *Escherichia coli* cells, buffer presented the rSpike protein (control 1), naïve control (not immunized), or a mix of two recombinant protein: PilZ protein from *Xanthomonas citri* and N-terminal part of perpetuity. LIC_11128 from *Leptospira interrogans* Copenhageni (control 2). Each group was performed using adult female fishes.

by physiological system. Animals that died during the injected experiment were excluded from the analysis.

2.5. Behavioral testing in adult

The *D. rerio*, 13 for the control and 17 for the spike group, were individualized in an aquarium (28 cm × 11 cm × 18 cm, length × width × height) without visual contact with other fish and left to habituate for one day. In the following day (day 2), fish locomotor activity was recorded (the camera was placed in the front of the test aquarium) 5 min before (baseline) and 30 min after the onset of alarm substance (AS) in the aquaria. A total of 0.4 ml of AS (see the section "Alarm substance" for further details on AS preparation) were administered through a plastic hose in the experimental aquaria, with a help of a syringe. A dark plastic tarp prevented fish to see the researcher applying the AS in the aquarium, avoiding any interference of the researcher in the fish's locomotor behavior. The side of the aquarium that the AS was inserted was randomized between the groups, to avoid any laterality effect in the results. All tests were realized between 8:00 h and 12:00 h, and the two treatments were intermixed throughout the day to account for possible diurnal variations in behavior.

The analysis of locomotor behavior was done using the ZebTrack software, developed at MatLab. The software is validated to analysis zebrafish locomotor behavior (Moura and Luchiari, 2016). The following locomotor behavior variables were assessed: time stopped, distance travelled, mean speed, maximum speed and distance from the bottom.

2.5.1. Alarm substance

The extraction followed the protocol described in Faustino et al. (2017). Eight adult zebrafish (4 males and 4 females) were individually collected from their tank, rinsed with distilled water, dried with paper towel, and sacrificed through the break of the spinal cord. Fourteen vertical and one horizontal shallow cuts were made in fish skin with surgical scalpel blade, at each side of the trunk. The cuts were washed with 50 mL of distilled water and then the solution was filtered, resulting in a 400 mL of AS solution that was divided into 4 mL aliquots. Then, the aliquots were stored at the freezer for posterior use in the experiments.

2.6. Ace2 expression by real-time quantitative PCR in adult zebrafish

Total RNA from brain, muscle, liver, kidney, heart, gonads (testis and ovary) from male and female zebrafish (n = 5 animals per sex) were extracted using the commercial PureLinkTM RNA Mini Kit (Ambion, CA, USA) according to manufacturer's instructions. The cDNA synthesis was performed as described by Nóbrega et al. (2010). The relative mRNA levels of ace2 (angiotensin I converting enzyme 2) was evaluated among different tissues of male and female zebrafish by real-time quantitative PCR (qPCR) using specific primers (forward: GACGGTTTTGGACCAACTTGT; reverse: TTTCATCCCAACCCTGCTCC). qPCR reactions were conducted using 5 μL 2× SYBR-Green Universal Master Mix, 1 μL of forward primer (9 mM), 1 μL of reverse primer (9 mM), 0.5 μL of Milli-Q® water and 2.5 μL of cDNA. The mRNA levels of the targets (Cts) were normalized by the reference gene β-actin (Tovo-Neto et al., 2020), according to the $2-(\Delta\Delta CT)$ method. Primers were designed based on zebrafish sequences available at Genbank (NCBI, https://www.ncbi.nlm.nih.gov/genbank/).

2.7. Bioinformatics in silico analysis

For *in silico* analysis, all FASTA sequences of proteins from zebrafish and human, and SARS-CoV-2 were downloaded from the UNIPROT database (http://www.uniprot.org). In addition, the percentage of similarity between the orthologous proteins of different species was calculated using the EMBOSS Water platform (https://www.ebi.ac.uk), and protein

alignments were performed using the ESPript platform (http://espript.ibcp.fr/ESPript/cgi708 bin/ESPript.cgi). For comparison of 3D structures, the FASTA files were converted into PDB files (containing the 3D coordinates of the proteins) using the Raptor X tool (http://raptorx.uchicago.edu). Then, structural similarities were compared on the iPDA platform (http://www.dsimb.inserm.fr), and structural images of proteins were done using the PyMOL software (https://pymol.org/2/). For the study of protein-protein interaction and Docking of Spike were performed using the Molsoft MolBrower 3.9-1b software.

2.8. Annotation of ontological data

The zebrafish and human proteins related to the subcellular location (cytoplasm, membrane, and nucleus) were recovered according to the annotation of ontological data in the ENSEMBL database (https://www.ensembl.org/index.html) For each subcellular location, protein-protein interactions were predicted with a SARS-CoV-2 Spike N-terminal fragment, residues 16–165, (rSpike) using the UNISPPI predictor, where only interactions with a score greater than 0.95 were accepted as interaction. The interacted proteins were submitted to functional enrichment to identify biological pathways using the G:Profiler software, based on the database of zebrafish and human. In addition, the proteins were analyzed with the Bioconductor Pathview package in the R environment in search of the biological pathways. The pathways were obtained from the Kyoto Encyclopedia of Genes and Genomes (KEGG) database and the model organism selected was the zebrafish and human.

2.9. Network analysis

Samples were analyzed in triplicate, and their molecular masses and isoelectric points of the proteins identified by MS/MS were observed using the ProtParam tool (http://us.expasy.org/tools/protparam.html). Data normalization was performed, and a significance cutoff was applied for the identified proteins at log-fold change ± 1.0. Subsequently, the identified proteins on the UniprotKB database were blasted against zebrafish. All data obtained were mapped using STRING web tool v11.0 (https://string696db.org/) to screen for protein-protein interactions (PPI).

2.10. Data analysis

The statistical analysis of the behavioral tests in adult zebrafish was performed in the R environment (v3.6.0.). Data were checked for outliers through boxplot interquartile method (Speedie and Gerlai, 2008). All the response variables were log10 transformed. Firstly, the difference between the locomotor behavior (time stopped, distance travelled, mean speed, maximum speed, and distance from the bottom) among the treatments (control and spike) and sampling time points (baseline and the first 10 min after AS onset) including the interactions were examined through linear mixed-effect models. The variables “treatment” and “sampling time points” were set as fixed factors, while “fish” was included as a nested random factor. Secondly, we realized linear mixed-effect models identical to the described above but to compare different sampling time points – we compare the fish locomotor behavior of both treatments over 30 min after alarm substance onset (AS) in 10 min bins (0–10 min, 10–20 min and 20–30 min). Post-hoc comparisons were done using Tukey or Bonferroni tests ($p < 0.05$).

3. Results

3.1. rSpike protein of zebrafish had an impact on the survival rate

SARS-CoV-2 spike protein fragment was obtained by cloning the DNA fragment for the full-lenght S protein RNA isolated from the second Brazilian, followed by heterologous protein expression in *E. coli* and purification. SDS-PAGE of the total cell lysates (Fig. 1a, b) shows that, after induction of expression, the band at about 16 kDa, corresponding to molecular mass of SARS-CoV-2 spike protein fragment. We demonstrated that 16 kDa band was specifically recognized by the anti-HisTag antibody (Fig. 1b).

Two bioassays were carried out to analyze the toxicity of the rSpike. The first injection of the rSpike generated high toxicity to the fish (Fig. 1c). Therefore, the assay was repeated by adding different control groups to confirm whether the toxicity findings were specific to the rSpike (Fig. 1c). In the first bioassay, after the fish were injected with rSpike, the survival rate was 78.6% during the first seven days (Fig. 1). The lethality was significantly increased when compared to naive control and fish injected with protein buffer (control 1), where the survival rates were 100% and 90%, respectively (Fig. 1c). Nonetheless, after a second injection, the rSpike injected group maintained the plateau survival rate, with no further increase in lethality in the treated group. Therefore, a second assay was conducted by adding different control groups in order to confirm that the toxicity findings were specific to the rSpike, and also the presence of antigens was accessed. The Kaplan-Meier survival analysis confirmed rSpike injection presented a lower survival rate compared to the two previous controls used (Control naïve and protein buffer) and compared to females injected with *Escherichia coli* extract or a culture medium mixed of two purified recombinant proteins (PilZ protein from *Xanthomonas citri*, and a N-terminal fragment of LIC_11128 from *Leptospira interrogans* Copenhageni) (Control 2) (Fig. 1c). The survival rate was maintained after the second injection for the next seven days. The relative risk of death in the period studied between the groups was significant (chi square = 79.70; $p < 0.0001$).

3.2. Behavioral test in adult zebrafish

We tested zebrafish olfaction after applying the SARS-CoV-2 spike protein fragment, testing perception and response to a co-specific alarm substance (chemical communication that triggers anti-predatory behavior in fish). We applied the behavioral tests 7 days after spike injection. Firstly, we tested whether SARS-CoV-2 spike protein fragment alter the baseline and the post alarm substance (AS) locomotor behavior. We did not observe a significant effect of treatments (control vs spike) and the interaction between treatments and sample time points in any response variable of locomotor behavior (time stopped, distance travelled, mean speed, maximum speed and distance from the bottom, $p > 0.05$; Fig. 2). However, we observed a significant effect of sample time points in the time stopped ($F_{1,30} = 92.309$, $p < 0.001$), distance travelled ($F_{1,\ 29.898} = 8.052$, $p = 0.008$), mean speed ($F_{1,30} = 38.599$, $p < 0.001$), maximum speed ($F_{1,30} = 57.35$, $p < 0.001$) and distance from the bottom ($F_{1,\ 27.482} = 39.929$, $p < 0.001$) (Fig. 2).

We also measured the fish anti-predatory response after the AS application in the aquarium over 30 min, measuring the behaviors in three different sampling time points (0–10 min, 10–20 min and 20–30 min). Like the comparison between the baseline and post AS behavior, we did not observe a significant effect of treatments and the interaction between treatments and sample time points in any response variable of locomotor behavior ($p > 0.05$; Fig. 3). However, we observed a significant effect of sample time points in the time stopped ($F_{2,\ 49.053} = 13.032$, $p < 0.001$), distance travelled ($F_{2,57.629} = 18.828$, $p < 0.001$) and mean speed ($F_{2,\ 57.033} = 14.383$, $p < 0.001$). Fish spent more time stopped at 10–20 min ($p = 0.038$) and 20–30 min ($p = 0.003$) than at 0–10 min, and also travelled longer distances with a high mean speed at 0–10 min than at 10–20 min ($p < 0.001$) and 20–30 min ($p < 0.001$) (Fig. 3a, b and c). We did not observe a significant effect of sample time points in the maximum speed ($F_{2,\ 59.402} = 1.508$, $p = 0.23$) and distance from the bottom ($F_{2,\ 47.377} = 2.7448$, $p = 0.0745$) (Fig. 3d and e).

3.3. Histopathological changes in adult zebrafish

In general, it was observed several morphological alterations compatible with an undergoing inflammatory process in many tissues. Markedly, brain obtained from treated fishes showed an intense inflammatory infiltrate with presence of many macrophages after 7 days (Fig. 4C) and an

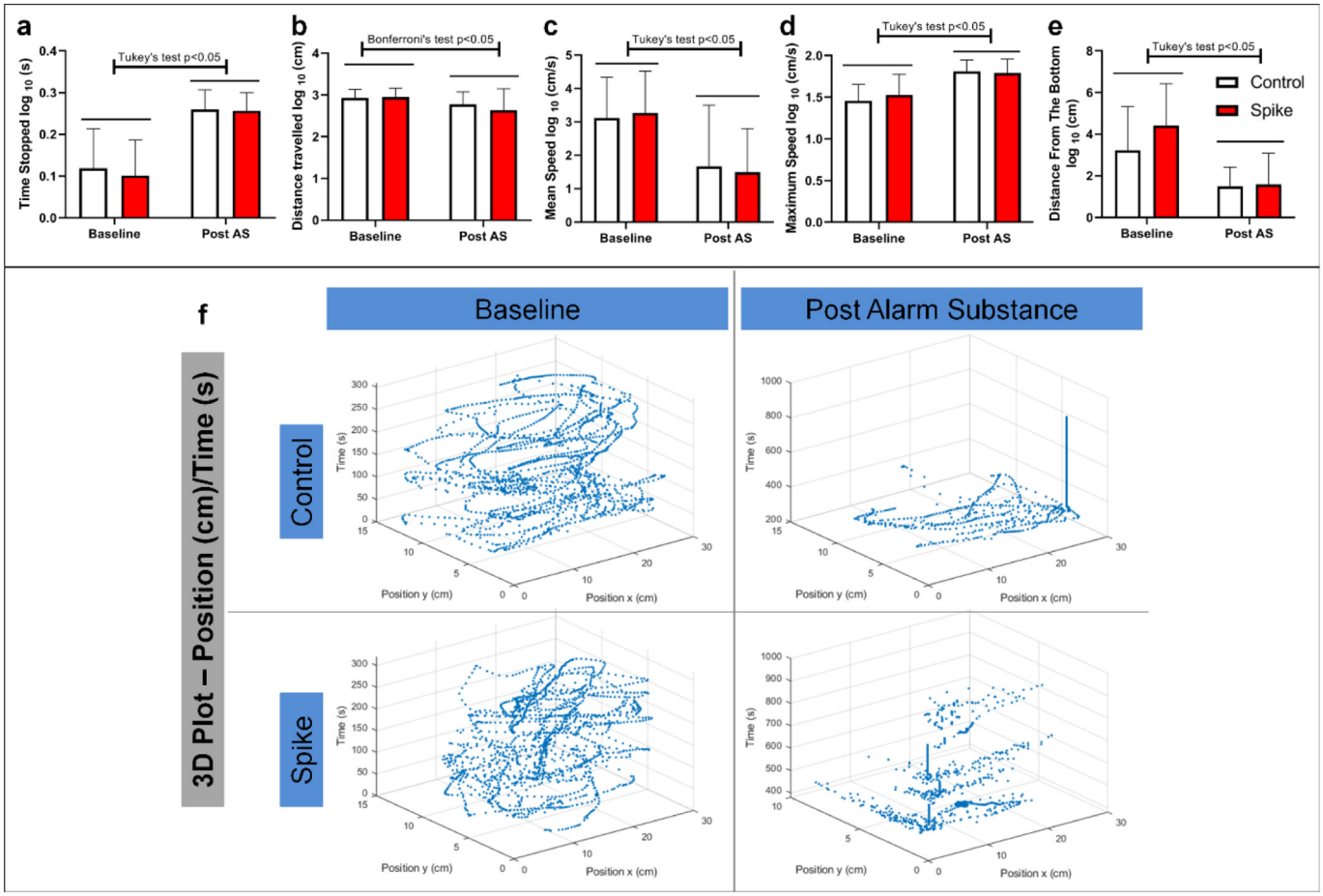

Fig. 2. Effect of spike infection in adult zebrafish locomotor behavior in two different sampling time points: baseline and the first 10 min after alarm substance (AS) onset. The following locomotor behavior variables were measured: (a) Time stopped, (b) distance travelled, (c) mean speed, (d) maximum speed and (e) distance from the bottom. All the response variables were Log10 transformed. $n = 13$ control and $n = 17$ spike. Mean ± SD are shown. Statistical difference between the groups in Tukey or Bonferroni post hoc tests are indicated in the graphs ($p < 0.05$). (f) 3D plots representative of each treatment (control and spike) in both sampling time points (baseline and post alarm substance). Each 3D plot represents the locomotor behavior of the zebrafish closest to the mean in each treatment.

intense mononuclear infiltrate after 14 days days (Fig. 4d and e). Histopathological analysis of the female reproductive tissue showed ovarian stroma with abundant and disorganized extracellular matrix (Fig. 4g). Follicular development showed alterations such as atresia among oocytes at primary growth and cortical alveolus stages (Fig. 4g). Moreover, dense inflammatory infiltrates are commonly seen in the ovarian stroma (Fig. 4h). On the other hand, the group of fish that received a second injection within the interval of 7 days showed no histological changes in their ovaries after 14 days, when compared to controls (Fig. 4i). In kidneys, we observed melanin and lipofuscin pigments, renal thrombosis and autophagy with tubular disarray and loss of tubular lumen epithelium, loss of Bowman's capsule space and the integrity of the glomerular tuft compromising blood filtration (Fig. 4n–o). The frequency of the relative systemic alterations is summarized in Table 1.

3.4. The human receptor angiotensin converting enzyme 2 (ACE2) share 72% sequence similarity to its ortholog in zebrafish and tissue distribution of zebrafish ACE2 mRNA

One of the known targets of SARS-CoV-2 Spike protein is the Angiotensin receptor converting enzyme 2 (ACE2) in humans. It is considered the main gateway to the virus infection. Considering the effects of rSpike protein on the fishes analyzed in this work, structural and functional similarities between zebrafish and human ACE2 were investigated, using bioinformatic analysis. Interestingly, zebrafish has ACE2 protein that shares 58 and 72% primary sequence identity and similarity to human ACE2, respectively (Figs. 5A; S2, see "Supplementary Material").

Human ACE2 interacts to the receptor binding domain (RBD) of SARS-CoV-2 Spike protein mainly by polar and salt bridge interactions. Human ACE2 has 22 residues making part of the protein-protein interaction and most of them are located at the N-terminal region of ACE2. 77% of the human ACE2 residues of the interface are similar in zebrafish ACE2 sequence (Figs. 5B; S2, see "Supplementary Material") suggesting that zebrafish may also binds SARS-CoV-2 Spike protein. The tree-dimensional structure of zebrafish ACE2 based on homology model (Fig. 5D) shows a high structural similarity with human ACE2. Computational analysis of protein-protein interaction using ACE2 and the RBD of SARS-CoV-2 Spike protein reveals similar values of binding free energy suggesting that zebrafish is susceptible to virus infection (Fig. 5c). In our work, we do not expect that rSpike protein interacts with zebrafish ACE2 because rSpike correspond to the N-terminal part of the Spike protein (residues 16–165) that precedes the RBD domain (residues 319–311,541).

Real-time, quantitative PCR analysis of several tissues from adult male and female zebrafish showed that ACE2 was predominantly expressed in the brain and muscle of both sexes (Fig. 5e). Although higher levels were seen in the kidney for females, the transcript abundance of ACE2 in this organ was quite variable and showed no significant differences when compared to other tissues (Fig. 5e). Further analysis compared the relative expression of zebrafish ACE2 between male and female for the same tissue. This analysis revealed higher expression of ACE2 in males than females for the following organs: brain, gonads, heart, muscle and adipose tissue (fat body) (Fig. 5E).

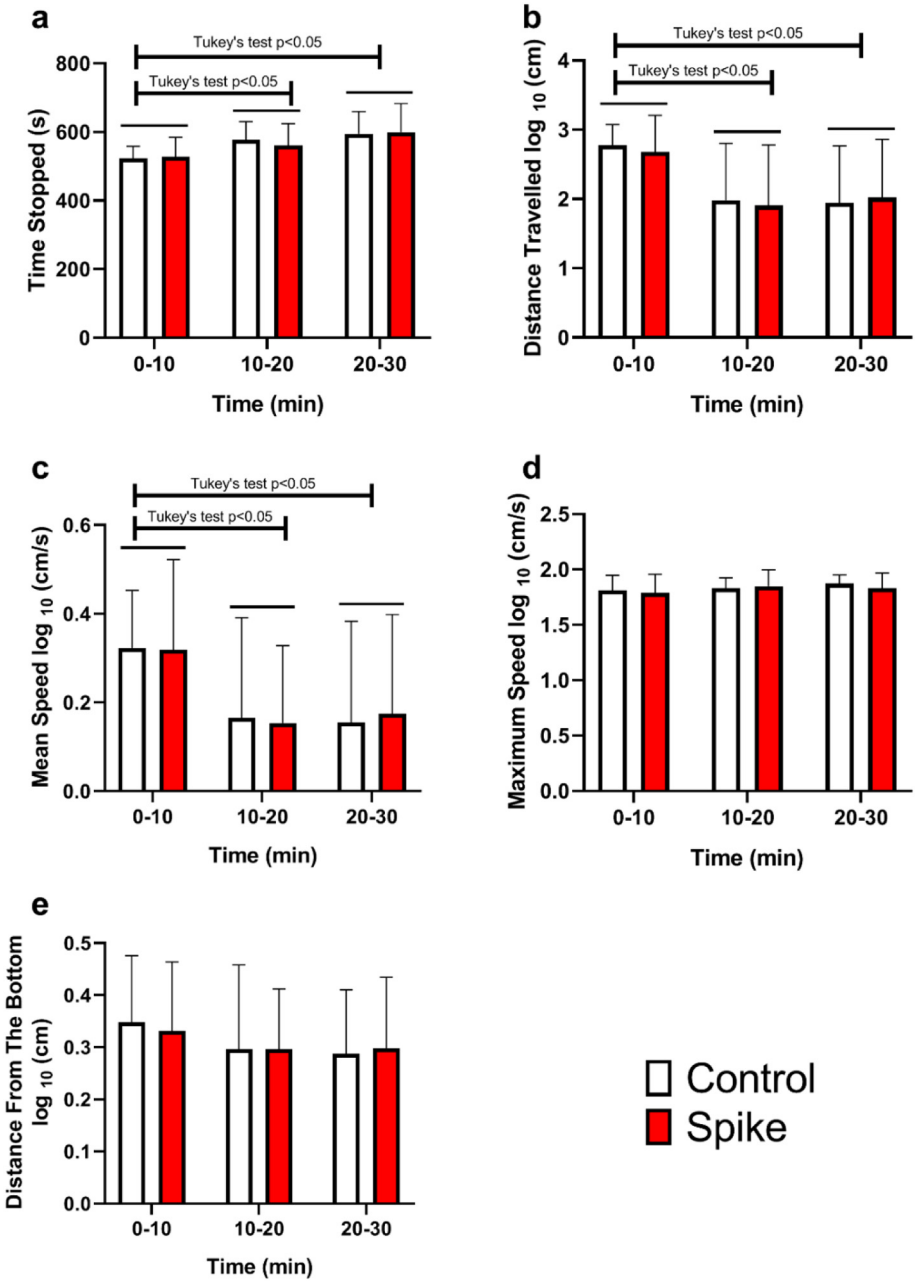

Fig. 3. Effect of spike injection in adult zebrafish locomotor behavior over 30 min after alarm substance onset (AS) in 10 min bins. The following locomotor behavior variables were measured: (a) time stopped, (b) distance travelled, (c) mean speed, (d) maximum speed and (e) distance from the bottom. All the response variables, except the time stopped, were log10 transformed. n = 13 control and n = 17 spike. Mean ± SD are shown. Statistical difference between the groups in Tukey post hoc test are indicated in the graphs ($p < 0.05$).

3.5. The protein-protein interaction prediction among SARS-CoV-2

The protein-protein interaction prediction among the rSpike and zebrafish proteins according to the subcellular location (membrane, cytoplasm, and nucleus) predicted interactions with 2910 proteins for the membrane, 771 proteins for the cytoplasm, and 1134 proteins for the nucleus. For human proteins and rSpike predicted interactions with 1785 proteins for the membrane, 1168 proteins for the cytoplasm, and 1242 proteins for the nucleus (Figs. S1 and S2, see "Supplementary Material"). Considering the most general ontological terms found hierarchically, according to the KEGG and Reactome databases, 71% of the terms identified for zebrafish are identical to those found for human. However, further analysis showed different specific terms with approximately 58% of different specific pathways. Functional enrichment of the biological pathways (zebrafish and human) showed basic processes related mainly to cell growth and death, including regulation of transcription and translation mechanisms, mechanisms of DNA repair or replication, and signaling pathways of p53 and by GPCR, among others. Additionally, we identified the pathways related to signal molecules and interactions, signal transduction, and the immune system (Fig. S2, see "Supplementary Material").

Interestingly, it was recovered through the protein-protein interaction with rSpike, the Toll-like receptor pathway (dre:04620 and hsa:04620). It can allow interaction with the Toll-like receptors TLR1, TLR2, TLR4, and TLR5 and the interferon-α/β receptor (IFNαβR), possibly triggering the activation of various signaling pathways (Fig. S3, see "Supplementary Material").

In this pathway, we observed a possible interaction of the rSpike with the signal transducer and activator of transcription 1-alpha/beta (STAT1)

protein in the cytoplasmic region. Additionally, the signal molecules and interaction pathway (zebrafish and human) showed the possibility of rSpike interacting with a considerable number of cell receptors related to the neuroactive ligand receptor (KEGG:4080) and a cytokine-cytokine receptor (Fig. S3, see "Supplementary Material") and triggering diverse cellular signaling such as the TGF beta signaling family, class I and II helical cytokines,

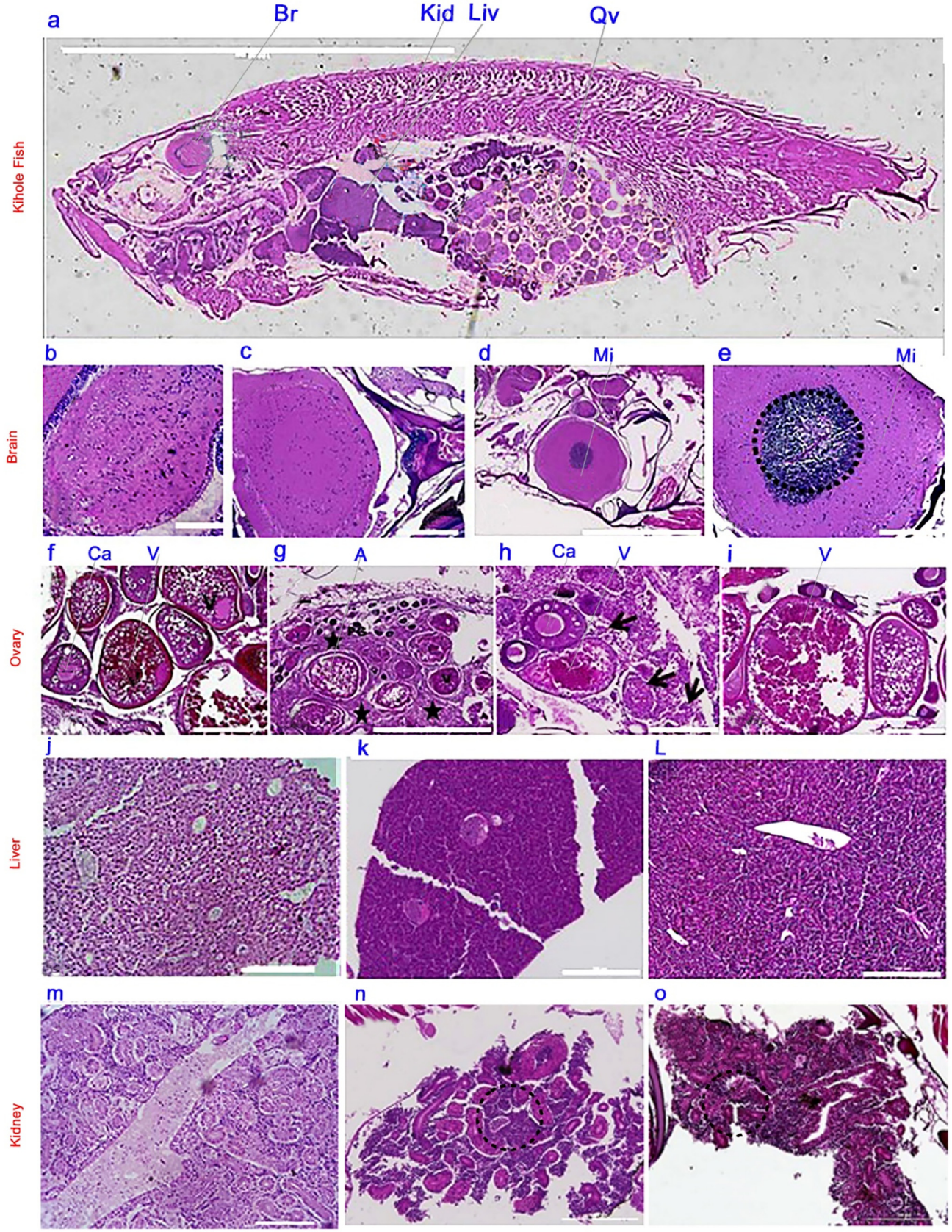

IL and TNF family. In addition, proteins related to the extracellular matrix, cellular communication and motility, formation of vesicles, transport and catabolism, VEGF signaling pathway, and AGE-RAGE signaling pathway in diabetic complications.

The possible virus-host protein interactions during the SARS-CoV-2 infection were tested in network analysis based on protein interactions (Fig. S4, see "Supplementary Material"). The important similarity between SARS-CoV-2 proteome and SARS-CoV proteome18 allowed us to hypothesize that the SARS-CoV proteome is highly conserved in SARS-CoV-2. In our network analysis, we were able to detect 29 proteins (Fig. S3, see "Supplementary Material") A PPI interaction database was assembled, including 7 nodes and 29 interactions. We analyzed the following proteins: Parvalbumin 4 (Pvalb4), Creatine kinase (Ckma), Keratin 5 (Krt5), A kinase anchor protein 1 (Ak1), Malate dehydrogenase (Mdh1aa), 2-phospho-D-glycerate hydro-lyase (Eno3), Component Chromosome 15 (ENSDARG00000095050), Component Chromosome 1 (wu:fk65c09), Component Chromosome 16 (Zgc:114037), Component Chromosome 17 9 Zgc:114046), Component Chromosome 26 (ENSDARG00000088889), Apolipoprotein A-II (Apoa2), Apolipoprotein A-Ib (Apoa1b), Serpin peptidase inhibitor member 7 (Serpina7), Transmembrane serine protease 2 (tmprss2), Fetuin B (fetub), Apolipoprotein A-I (apoa1a), Carboxylic ester hydrolase (ces3), Apolipoprotein Bb (apobb), tandem duplicate 1, Fibrinopeptide A (fga), Serotransferrin (tfa), Apolipoprotein C-I (apoc1), Complement component C9 (c9), Pentaxin (crp), Ceruloplasmin (cp), Hemopexin (hpx), Ba1 protein (ba1), Component Chromosome 13 (ENSDARG00000), and Component Chromosome 25 (ENSDARG0000008912).

4. Discussion

Here it was demonstrated, for the first time, that zebrafish injected with rSpike protein, fragment 16 to 165 (rSpike), that corresponds to the N-terminal portion of the protein, showed adverse effects on liver, kidney, nervous and reproduction system, using a series of experiments to validate zebrafish model for toxicological and pre-clinical safety studies with SARS-Cov-2.

Interestingly, fish injected with rSpike produced a toxic inflammatory response with similarity to severe cases of COVID-19 in humans (Fig. 2 and Table 1). Histological alterations were analyzed in the liver as mild lobular infiltration by small lymphocytes, centrilobular sinusoidal dilation, patchy necrosis, moderate microvesicular steatosis, mild inflammatory infiltrates in the hepatic lobule, and the portal tract. These changes are similar to those observed in patients with COVID-19 (Tian et al., 2020). Although the zebrafish biochemical liver function was not tested, a three-fold increase in ALT, AST, and GGT levels has been reported during hospitalization for humans. These alterations could be related to the direct cytopathic effect of the virus and could be associated with higher mortality (Jothimani et al., 2020).

With respect to the reproductive tissue, female zebrafish injected with rSpike displayed severe damage in the ovary (follicular atresia, cellular infiltration, and disorganized extracellular matrix) after 7 days of protein inoculation. On the other hand, it is remarkable that ovarian damage was reversed after 14 days, when zebrafish received a second injection of rSpike. In humans, there is evidence that ACE2 mRNA is expressed, at low levels, during all stages of follicle maturation in the ovary (Reis et al., 2011), and also in the endometrium (Vaz-Silva et al., 2009). This pattern of ACE2 expression, in line with our observations, could suggest that SARS-CoV-2 affects female fertility in humans and zebrafish. More studies will be necessary to comprehend the molecular mechanisms underlying SARS-CoV-2-induced female infertility and the effects in the ovarian function. To date, damage in the female reproductive system of COVID-19 patients has not been reported yet (Zupin et al., 2020).

Other different systems were affected, including the nervous system. In fact, some recent studies have reported that the SARS-CoV-2 may affect the nervous system (Cavalcanti et al., 2020; Iadecola et al., 2020; Lu et al., 2020) as the peripheral nervous system (Lau et al., 2004; Netland et al., 2008; Tian et al., 2020), particularly in the most severe cases of infection (Beghi et al., 2020). In our study, the rSpike was responsible for generating an inflammatory process in the brain (Fig. 4e), characterized by an intense influx of mononuclear cells, but no histopathological lesions, these inflammatory infiltrate findings were confirmed by immunohistochemical analysis. This profile is in line with the clinical reports of COVID-19 associated acute necrotizing myelitis (Sotoca and Rodríguez-Álvarez, 2020), where lymphocytic pleocytosis was observed in the cerebrospinal fluid (CSF). Acute transverse myelitis related to SARS-CoV-2 infection (Munz et al., 2020), where an intense leukocyte infiltrate of monocytic characteristic and elevated protein level was also observed in the CSF.

In another report, thrombosis in superficial and deep systems, straight sinus, the vein of Galen, internal cerebral veins. The application of spike in zebrafish's olfactory epithelium causes thrombosis of the deep medullary veins (Cavalcanti et al., 2020). Damage to the structure and function of this system can lead to severe encephalitis, toxic encephalopathy, and, after viral infections, severe acute demyelinating lesions (Wright et al., 2008). In a case study of 4 children with COVID-19, Abdel-Mannan et al. (2020) reported that children with COVID-19 may have late neurological symptoms. According to these findings, a recent work published by Rhea et al. demonstrated that the protein S of SARS-CoV2 is able to cross the blood-brain barrier in experimental murine models (Rhea et al., 2021). More interestingly, the work demonstrated that the phenomenon is mediated by the expression of ACE-2 in the cerebral microvasculature, and its transport to the brain parenchyma is via transcytosis. Therefore, these findings corroborate the hypothesis that not only does SARS-CoV2 have neurotropism, but that the Spike protein and the S1 protein of SARS-CoV-2 crosses the blood-brain barrier in mice. Future studies with zebrafish might provide more information about the virus damage in the nervous system.

Nonetheless, these alterations in the nervous system did not reflect in an alteration in the baseline locomotor behavior of adult zebrafish females (Fig. 2). Indeed, the observed alterations in the nervous system in the present study did not impair the perception and the response to a co-specific alarm substance (chemical communication that triggers anti-predatory behavior in fish). Basically, both the control and the infected group triggered all the anti-predatory behaviors considered standards of the species after the application of the alarm substance in the aquariums (Figs. 2 and 3). A recent study (Kraus et al., 2020) showed that the application of spike in the olfactory epithelium of zebrafish causes damage to the olfactory epithelium in the period immediately after application, up to 5 days. The fish in that study did not respond to chemical stimuli from food and bile, 3 h after infection and 1 day after. One possible explanation to this divergence between present results and Kraus et al. (2020), is the time that fish were tested after spike infection. We did the behavioral tests 7 days after spike injection, so, we may have caught the regeneration phase of this tissue. Another possible explanation for the difference in the results between these studies, is the difference between the chemical stimuli used, Kraus et al.

Fig. 4. Histopathological changes in adult zebrafish. a: longitudinal section of the whole female zebrafish for morphological analyses of the main organs affected. All sections were stained with Hematoxylin Eosin. Brain: (b)- histology of control, (c)- brain histology after 7 days of first injected presenting macrophages, and (d) 14 days after first injected with a burst after 7 days from the first injected presenting intense mononuclear infiltrate. (e) The same image as panel d but at a higher magnification. Ovary: ovarian histology from zebrafish control (f), after 7 (g–h) and 14 days (i). (f–i) Follicular development was classified as primary growth oocyte (PG), cortical alveolus (CA), and vitellogenic (V) stages. Asterisks in panel g indicate an abundant and disorganized extracellular matrix in the ovarian stroma. (h) Inset shows a higher magnification of the cellular infiltration and arrows show dense, eosinophilic inflammatory infiltrates. (i) The histology of ovaries after 14 days is similar to the control. Scale bars: 1000 μm (g) and 200 μm (f, h, and i). Liver: Histology of the liver from control (j), after 7 days from rSpike injected (l), and after 14 days from the first injected with a burst at 7 days (m). Kidney: histology of kidney from zebrafish control (n), after 7 days from the first injected (o), and after 14 days from the first injected with a second injected after 7 days (p). Scale bars: 1000 μm (n) and 200 μm (o–p).

Table 1
Summary of histopathological findings in different organs of zebrafish injected with rSpike. Number of female fish with histopathological alterations out of total female fish injected. Females were injected either with Naïve control ($n = 5$), control 1 (protein buffer) ($n = 5$), or SARS-CoV-2 rSpike ($n = 20$).

System	Organs	Changes/pathology	NAIVE	Control 1	SARS-CoV2 rSpike
Circulatory	Heart	Lymphoid foci	0/5	0/5	1/20
	Kidney	Renal thrombosis	0/5	0/5	2/20
	Liver	Hyperemia	0/5	1/5	2/20
	Spleen	Hyperemia	0/5	0/5	0/20
Reproductive	Ovary	Atresic follicles	0/5	1/5	6/20
Nervous	Brain	Lymphoid foci	0/5	0/5	3/20
Digestive	Intestine	–	0/5	0/5	1/20
Urinary	Kidney	Presence of pigments, tubular and Bowman capsule structural integrity loss	0/5	0/5	2/20
Fotoreceptor	Eye	–	0/5	0/5	0/20
Endocrine	Langehans islands	–	0/5	0/5	0/20
Tegumentar	–	–	0/5	0/5	0/20
Respiratory	Gills	–	0/5	0/5	0/20

(2020) used food and bile as chemical stimuli, and in the present work, it was used an AS obtained from the skin damaged fishes, mimetizing the natural phenomena, where damaged fishes released AS, inducing fear and anti-predatory responses in other neighboring fish that perceive the signal (Speedie and Gerlai, 2008). Anti-predatory response is so evolutionarily conserved that even with the damaged olfactory epithelium (as well as the ability to capture very little of the alarm substance's stimulus), a low uptake of stimulation of the alarm substance is enough to trigger an anti-predatory response. Thus, the spike can impair the perception of more specific chemical signals including food and bile, as shown by Kraus et al. (2020), but not when these signals trigger a response to a life or death threat, as in the case of the alarm substance. Another possibility is that physical limitation of olfactory tissue in zebrafish impairs COVID protein biding to target host cells but allows protein fragments to affect the host cells. Comparing protein versus fragments effect in zebrafish, we hypothesize that, when an organism is injected with SARS-CoV-2, the virus releases fragment(s) of the spike protein that can target host cells for eliciting cell signaling without the rest of the viral components. Thus, zebrafish subjected to the intact virus infecting the host cells for the replication and amplification as well as the spike protein fragments that are capable of affecting the host cells. It was hypothesized that cell signaling elicited by the spike protein fragments that occur in cells would predispose injected individuals to develop complications that are seen in severe and fatal COVID-19 conditions. If this hypothesis is correct, then the strategies to treat COVID-19 should include, in addition to agents that inhibit the viral replication, therapeutics that inhibit the viral protein fragment-mediated cell signaling.

In the sequence of these experimental findings, the in silico analysis showed that zebrafish ACE2 receptor has the same potential for protein-ligand interaction as in humans (Fig. 5). We show in silico and in vivo that the zebrafish ACE2 receptor is susceptible to the rSpike and interacts similarly to the human ACE2 receptor. The importance of ACE2 receptor for SARS-CoV-2 infection and its role in vaccine studies is shown in research with transgenic mice (HFH4-hACE2 in C3B6 mice) (Jiang et al., 2020). The use of perpetuity ACE2 receptor by SARS-CoV-2 in the attachment and infection of the host cells has been well postulated in mammals, except for

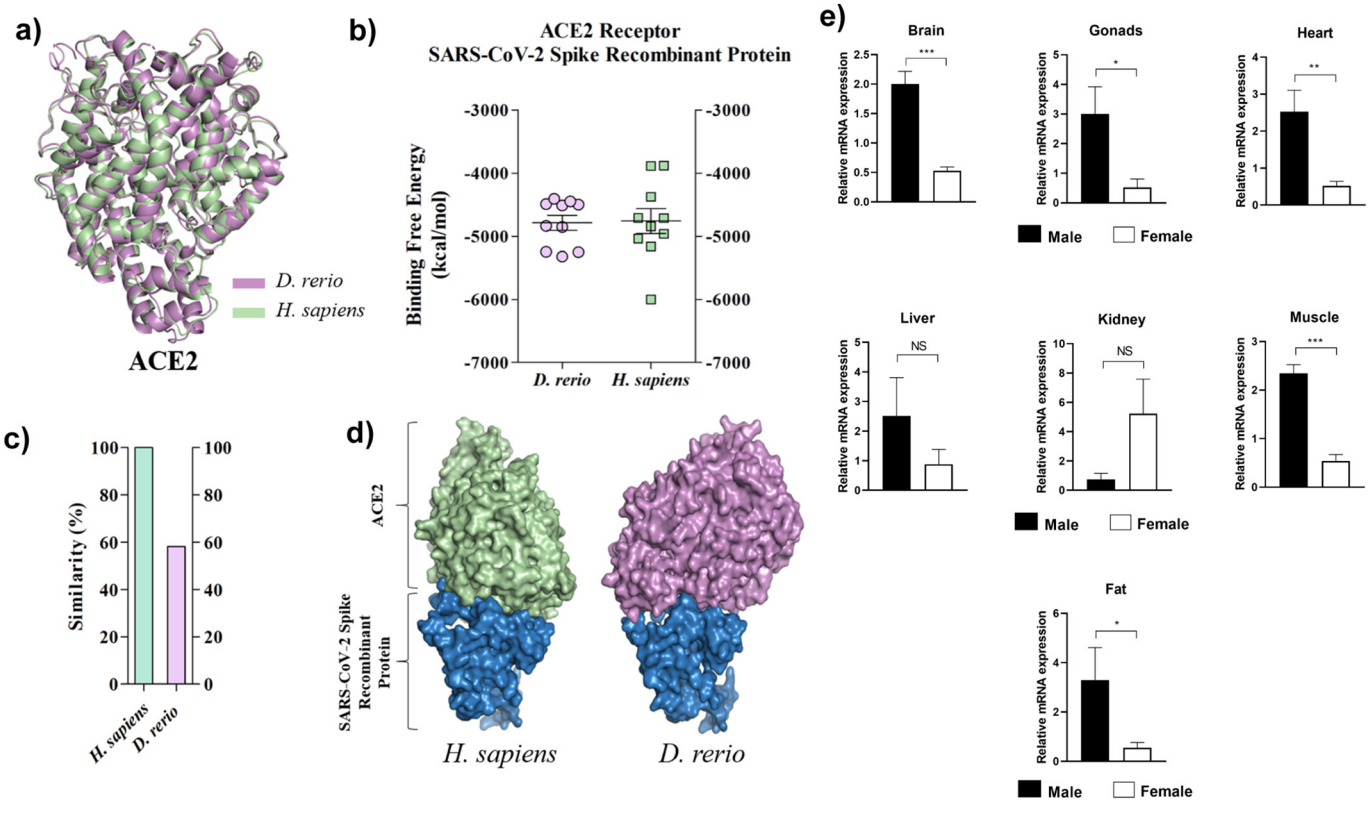

Fig. 5. In silico analysis of the interaction of the human and zebrafish ACE2 receptor with rSpike protein. (a) Structural alignment between ACE2 of human and zebrafish. For comparison of 3D structures, the FASTA files were converted into PDB files (containing the 3D coordinates of the proteins) using the Raptor X tool (http://raptorx.uchicago.edu). (b) Graphs show the free binding energy in protein-ligand interactions docking analysis and the axis (X) represents the score of 10 (ten) possibilities of interaction between molecule-ligand and the axis (Y) compares the free binding energy it represents per kilocalorie per mol (Kcal/mol). (Kcal/mol). (c) The similarity of ACE2 between human and zebrafish. (d) Protein-protein interaction between human and zebrafish ACE2 and SARS-CoV-2 Spike RBD. (e) Relative expression of ACE2 mRNA in zebrafish adult organs (n = 5 males; n = 5 females). Values represent mean ± SEM. Asterisks indicate a significant difference between male and female; ***$p < 0.001$; **$p < 0.01$; *$p < 0.05$; NS = not significant.

murines, and some birds, such as pigeons (Qiu et al., 2020). The ACE-2 orthologue studies in non-mammalian animals, including zebrafish, suggest the potential to unveil the role of this enzyme and its use for therapeutic purposes (Chou et al., 2006).

5. Conclusions

Our studies reveled that zebrafish showed inflammatory reaction to SARS-CoV-2 rSpike protein which provoked damage to organs (liver, kidney, ovaries and brain) in a similar pattern as happen in severe cases of COVID-19 in humans and resulted in 78,6% of survival rate in female adults during the first seven days. The application of spike protein in zebrafish was highly toxic that is suitable for future studies to gather valuable information about ecotoxicological impacts, as well as vaccine responses and therapeutic approaches in human medicine. Therefore, besides representing an important tool to assess the harmful effects of SARS-CoV-2 in the aquatic environment, we present the zebrafish as an animal model for translational COVID-19 research.

Supplementary data to this article can be found online at https://doi.org/10.1016/j.scitotenv.2021.152345.

Declaration of competing interest

The authors declare that they have no known competing financial interests or personal relationships that could have appeared to influence the work reported in this paper.

Acknowledgment

This work was supported by São Paulo Research Foundation (FAPESP 2020/05761-3), Brazilian National Research Council (CNPq) (426531/2018-3) and *Instituto Federal Goiano* for the financial support Malafaia G. holds productivity scholarship from CNPq (307743/2018-7). Financial and material support was provided through the São Paulo Research 526 Foundation (FAPESP) granted to: Ives Charlie: Fapesp #2018/07098-0; 2019/19939-1; 527 Cristiane Rodrigues Guzzo: Fapesp #2019/00195-2, 2020/04680-0; Chuck Farah: Fapesp #2017/17303-7; Germán G. Sgro: Fapesp #2014/04294-1; Edgar E. Llontop: Fapesp #2019/12234-2; Natalia F. Bueno: Fapesp #2019/18356-2; Camila G. Bomfim: Fapesp #2019/21739-0. LJGB is supported by a research fellowship from Conselho Nacional de Desenvolvimento Científico e Tecnológico, Brazil (CNPq) 303263/2018-0 and FIFG has a PhD fellowship from FAPESP (2019/14285-3). Rede Virus MCTI (grant FINEP 0459/20), We would like to thank the Medical School Foundation for financial support (Project CG 19,110). We would also like to thank the entire organizing team of the Global Virtual Hackathon 2020 for the award our team received and the support from the Ministry of Transport, Communications and High Technologies of the Republic of Azerbaijan, the United Nations Development Program, and the SUP.VC Acceleration Center. Authors are also thankful to Sartorius for technical support in this work.

References

Abdel-Mannan, O., Eyre, M., Löbel, U., Bamford, A., Eltze, C., Hameed, B., Hacohen, Y., 2020. Neurologic and radiographic findings associated with COVID-19 infection in children. JAMA Neurol. https://doi.org/10.1001/jamaneurol.2020.2687.

Abu-Qdais, H.A., Al-Ghazo, M.A., Al-Ghazo, E.M., 2020. Statistical analysis and characteristics of hospital medical waste under novel Coronavirus outbreak. Glob. J. Environ. Sci. Manag. 6 (Special Issue), 21–30. https://doi.org/10.22034/GJESM.2019.06.SI.03.

Adhikari, S.P., Meng, S., Wu, Y.-J., Mao, Y.-P., Ye, R.-X., Wang, Q.-Z., Zhou, H., 2020. Epidemiology, causes, clinical manifestation and diagnosis, prevention and control of coronavirus disease (COVID-19) during the early outbreak period: a scoping review. Infect. Dis. Poverty 9 (1), 29. https://doi.org/10.1186/s40249-020-00646-x.

Bangaru, S., Ozorowski, G., Turner, H.L., Antanasijevic, A., Huang, D., Wang, X., Ward, A.B., 2020. Structural analysis of full-length SARS-CoV-2 spike protein from an advanced vaccine candidate. Science 370 (6520), 1089–1094. https://doi.org/10.1126/science.abe1502.

Beghi, E., Feigin, V., Caso, V., Santalucia, P., Logroscino, G., 2020. COVID-19 infection and neurological complications: present findings and future predictions. Neuroepidemiology 1–6. https://doi.org/10.1159/000508991.

Cavalcanti, D.D., Raz, E., Shapiro, M., Dehkharghani, S., Yaghi, S., Lillemoe, K., Nelson, P.K., 2020. Cerebral venous thrombosis associated with COVID-19. Am. J. Neuroradiol. 41 (8), 1370–1376. https://doi.org/10.3174/ajnr.A6644.

Chou, C.F., Loh, C.B., Foo, Y.K., Shen, S., Fielding, B.C., Tan, T.H.P., Fu, J., 2006. ACE2 orthologues in non-mammalian vertebrates (Danio, Gallus, Fugu, Tetraodon and Xenopus). Gene 377 (1–2), 46–55. https://doi.org/10.1016/j.gene.2006.03.010.

Coughlan, L., 2020. Snatching the crown from SARS-CoV-2. Cell Host Microbe 28 (3), 360–363. https://doi.org/10.1016/j.chom.2020.08.007.

Elsamadony, M., Fujii, M., Miura, T., Watanabe, T., 2021. Possible transmission of viruses from contaminated human feces and sewage: implications for SARS-CoV-2. Sci. Total Environ. 755, 142575. https://doi.org/10.1016/j.scitotenv.2020.142575.

Fan, L., Wang, Y., Jiang, N., Gao, L., Li, K., Gao, Y., Qi, X., 2020. A reassortment vaccine candidate of the novel variant infectious bursal disease virus. Vet. Microbiol. 251, 108905. https://doi.org/10.1016/j.vetmic.2020.108905.

Faustino, A.I., Tacão-Monteiro, A., Oliveira, R.F., 2017. Mechanisms of social buffering of fear in zebrafish. Sci. Rep. 7 (1), 44329. https://doi.org/10.1038/srep44329.

Gautam, R., Sharma, M., 2020. 2019-nCoV pandemic: a disruptive and stressful atmosphere for indian academic fraternity. Brain Behav. Immun. 88, 948–949. https://doi.org/10.1016/j.bbi.2020.04.025.

Guzzo, C.R., Salinas, R.K., Andrade, M.O., Farah, C.S., 2009. PILZ protein structure and interactions with PILB and the FIMX EAL domain: implications for control of type IV pilus biogenesis. J. Mol. Biol. 393 (4), 848–866.

Harrison, A.G., Lin, T., Wang, P., 2020. Mechanisms of SARS-CoV-2 transmission and pathogenesis. Trends Immunol. 41 (12), 1100–1115. https://doi.org/10.1016/j.it.2020.10.004.

Hoffmann, M., Kleine-Weber, H., Schroeder, S., Krüger, N., Herrler, T., Erichsen, S., Pöhlmann, S., 2020. SARS-CoV-2 cell entry depends on ACE2 and TMPRSS2 and is blocked by a clinically proven protease inhibitor. Cell 181 (2), 271–280.e8. https://doi.org/10.1016/j.cell.2020.02.052.

Iadecola, C., Anrather, J., Kamel, H., 2020. Effects of COVID-19 on the nervous system. Cell https://doi.org/10.1016/j.cell.2020.08.028.

Jiang, R.-D., Liu, M.-Q., Chen, Y., Shan, C., Zhou, Y.-W., Shen, X.-R., Shi, Z.-L., 2020. Pathogenesis of SARS-CoV-2 in transgenic mice expressing human angiotensin-converting enzyme 2. Cell 182 (1), 50–58.e8. https://doi.org/10.1016/j.cell.2020.05.027.

Jones, D.L., Baluja, M.Q., Graham, D.W., Corbishley, A., McDonald, J.E., Malham, S.K., Farkas, K., 2020. Shedding of SARS-CoV-2 in feces and urine and its potential role in person-to-person transmission and the environment-based spread of COVID-19. Sci. Total Environ. 749, 141364. https://doi.org/10.1016/j.scitotenv.2020.141364.

Jothimani, D., Venugopal, R., Abedin, M.F., Kaliamoorthy, I., Rela, M., 2020. COVID-19 and the liver. J. Hepatol. https://doi.org/10.1016/j.jhep.2020.06.006.

Kampf, G., Todt, D., Pfaender, S., Steinmann, E., 2020. Persistence of coronaviruses on inanimate surfaces and their inactivation with biocidal agents. J. Hosp. Infect. 104 (3), 246–251. https://doi.org/10.1016/j.jhin.2020.01.022.

Keech, C., Albert, G., Cho, I., Robertson, A., Reed, P., Neal, S., Glenn, G.M., 2020. Phase 1–2 trial of a SARS-CoV-2 recombinant spike protein nanoparticle vaccine. N. Engl. J. Med. 383 (24), 2320–2332. https://doi.org/10.1056/NEJMoa2026920.

Kraus, A., Casadei, E., Huertas, M., Ye, C., Bradfute, S., Levraud, J., Salinas, I., 2020. Cardiovascular.

Lan, J., Ge, J., Yu, J., Shan, S., Zhou, H., Fan, S., Wang, X., 2020. Structure of the SARS-CoV-2 spike receptor-binding domain bound to the ACE2 receptor. Nature 581 (7807), 215–220. https://doi.org/10.1038/s41586-020-2180-5.

Lau, K.-K., Yu, W.-C., Chu, C.-M., Lau, S.-T., Sheng, B., Yuen, K.-Y., 2004. Possible central nervous system infection by SARS coronavirus. Emerg. Infect. Dis. 10 (2), 342–344. https://doi.org/10.3201/eid1002.030638.

Liu, D., Thompson, J.R., Carducci, A., Bi, X., 2020. Potential secondary transmission of SARS-CoV-2 via wastewater. Sci. Total Environ. 749, 142358. https://doi.org/10.1016/j.scitotenv.2020.142358.

Lu, Y., Li, X., Geng, D., Mei, N., Wu, P.-Y., Huang, C.-C., Yin, B., 2020. Cerebral microstructural changes in COVID-19 patients – an MRI-based 3-month follow-up study. EClinicalMedicine 25, 100484. https://doi.org/10.1016/j.eclinm.2020.100484.

McKibbin, W.J., Fernando, R., 2020. The global macroeconomic impacts of COVID-19: seven scenarios. SSRN Electron. J. https://doi.org/10.2139/ssrn.3547729.

Meyerowitz, E.A., Richterman, A., Gandhi, R.T., Sax, P.E., 2021. Transmission of SARS-CoV-2: a review of viral, host, and environmental factors. Ann. Intern. Med. 174 (1), 69–79. https://doi.org/10.7326/M20-5008.

Moghadas, S.M., Fitzpatrick, M.C., Sah, P., Pandey, A., Shoukat, A., Singer, B.H., Galvani, A.P., 2020. The implications of silent transmission for the control of COVID-19 outbreaks. Proc. Natl. Acad. Sci. 117 (30), 17513–17515. https://doi.org/10.1073/pnas.2008373117.

Moore, J.L., Aros, M., Steudel, K.G., Cheng, K.C., 2002. Fixation and decalcification of adult zebrafish for histological, immunocytochemical, and genotypic analysis. BioTechniques 32 (2), 296–298. https://doi.org/10.2144/02322st03.

Moura, C.de A., Luchiari, A.C., 2016. Time-place learning in the zebrafish (Danio rerio). 128, 64–69. https://doi.org/10.1016/j.beproc.2016.04.007.

Munz, M., Wessendorf, S., Koretsis, G., Tewald, F., Baegi, R., Krämer, S., Reinhard, M., 2020. Acute transverse myelitis after COVID-19 pneumonia. J. Neurol. 267 (8), 2196–2197. https://doi.org/10.1007/s00415-020-09934-w.

Netland, J., Meyerholz, D.K., Moore, S., Cassell, M., Perlman, S., 2008. Severe acute respiratory syndrome coronavirus infection causes neuronal death in the absence of encephalitis in mice transgenic for human ACE2. J. Virol. 82 (15), 7264–7275. https://doi.org/10.1128/JVI.00737-08.

Nóbrega, R.H., Greebe, C.D., van de Kant, H., Bogerd, J., de França, L.R., Schulz, R.W., 2010. Spermatogonial stem cell niche and spermatogonial stem cell transplantation in zebrafish. PLoS ONE 5 (9), e12808. https://doi.org/10.1371/journal.pone.0012808.

Qiu, Y., Zhao, Y.-B., Wang, Q., Li, J.-Y., Zhou, Z.-J., Liao, C.-H., Ge, X.-Y., 2020. Predicting the angiotensin converting enzyme 2 (ACE2) utilizing capability as the receptor of SARS-CoV-2. Microbes Infect. 22 (4–5), 221–225. https://doi.org/10.1016/j.micinf.2020.03.003.

Ravichandran, S., Coyle, E.M., Klenow, L., Tang, J., Grubbs, G., Liu, S., Khurana, S., 2020. Antibody signature induced by SARS-CoV-2 spike protein immunogens in rabbits. Sci. Transl. Med. 12 (550), eabc3539. https://doi.org/10.1126/scitranslmed.abc3539.

Reis, F.M., Bouissou, D.R., Pereira, V.M., Camargos, A.F., dos Reis, A.M., Santos, R.A., 2011. Angiotensin-(1–7), its receptor mas, and the angiotensin-converting enzyme type 2 are expressed in the human ovary. Fertil. Steril. 95 (1), 176–181. https://doi.org/10.1016/j.fertnstert.2010.06.060.

Rhea, E.M., Logsdon, A.F., Hansen, K.M., Williams, L.M., Reed, M.J., Baumann, K.K., Erickson, M.A., 2021. The S1 protein of SARS-CoV-2 crosses the blood–brain barrier in mice. Nat. Neurosci. 24 (3), 368–378. https://doi.org/10.1038/s41593-020-00771-8.

Samrat, S.K., Tharappel, A.M., Li, Z., Li, H., 2020. Prospect of SARS-CoV-2 spike protein: potential role in vaccine and therapeutic development. Virus Res. 288, 198141. https://doi.org/10.1016/j.virusres.2020.198141.

Sangkham, S., 2020. Face mask and medical waste disposal during the novel COVID-19 pandemic in Asia. Case Stud. Chem. Environ. Eng. 2, 100052. https://doi.org/10.1016/j.cscee.2020.100052.

Shang, J., Ye, G., Shi, K., Wan, Y., Luo, C., Aihara, H., Li, F., 2020. Structural basis of receptor recognition by SARS-CoV-2. Nature 581 (7807), 221–224. https://doi.org/10.1038/s41586-020-2179-y.

Sotoca, J., Rodríguez-Álvarez, Y., 2020. COVID-19-associated acute necrotizing myelitis. Neurol.Neuroimmunol. Neuroinflamm. 7 (5), e803. https://doi.org/10.1212/NXI.0000000000000803.

Speedie, N., Gerlai, R., 2008. Alarm substance induced behavioral responses in zebrafish (Danio rerio). Behav. Brain Res. 188 (1), 168–177. https://doi.org/10.1016/j.bbr.2007.10.031.

Sun, J., Zhu, A., Li, H., Zheng, K., Zhuang, Z., Chen, Z., Li, Y., 2020. Isolation of infectious SARS-CoV-2 from urine of a COVID-19 patient. Emerg. Microbes Infect. 9 (1), 991–993. https://doi.org/10.1080/22221751.2020.1760144.

Tian, S., Xiong, Y., Liu, H., Niu, L., Guo, J., Liao, M., Xiao, S.Y., 2020. Pathological study of the 2019 novel coronavirus disease (COVID-19) through postmortem core biopsies. Mod. Pathol. 33 (6), 1007–1014. https://doi.org/10.1038/s41379-020-0536-x.

Tovo-Neto, A., Martinez, E.R.M., Melo, A.G., Doretto, L.B., Butzge, A.J., Rodrigues, M.S., Nóbrega, R.H., 2020. Cortisol directly stimulates spermatogonial differentiation, meiosis, and spermiogenesis in zebrafish (Danio rerio) testicular explants. Biomolecules 10 (3), 429. https://doi.org/10.3390/biom10030429.

Tsang, B., Zahid, H., Ansari, R., Lee, R.C.-Y., Partap, A., Gerlai, R., 2017. Breeding zebrafish: a review of different methods and a discussion on standardization. Zebrafish 14 (6), 561–573. https://doi.org/10.1089/zeb.2017.1477.

Teymoorian, T., Teymourian, T., Kowsari, E., Ramakrishna, S., 2021. Direct and indirect effects of SARS-CoV-2 on wastewater treatment. J. Water Process. Eng. 42, 102193.

Urban, R.C., Nakada, L.Y.K., 2021. COVID-19 pandemic: solid waste and environmental impacts in Brazil. Sci. Total Environ. 755, 142471. https://doi.org/10.1016/j.scitotenv.2020.142471.

Vaz-Silva, J., Carneiro, M.M., Ferreira, M.C., Pinheiro, S.V.B., Silva, D.A., Silva, A.L., Reis, F.M., 2009. The vasoactive peptide angiotensin-(1–7), its receptor Mas and the angiotensin-converting enzyme type 2 are expressed in the human endometrium. Reprod. Sci. 16 (3), 247–256. https://doi.org/10.1177/1933719108327593.

Wang, H., Zhang, Y., Huang, B., Deng, W., Quan, Y., Wang, W., Yang, X., 2020. Development of an inactivated vaccine candidate, BBIBP-CorV, with potent protection against SARS-CoV-2. Cell 182 (3), 713–721.e9. https://doi.org/10.1016/j.cell.2020.06.008.

Wang, J., Shen, J., Ye, D., Yan, X., Zhang, Y., Yang, W., Pan, L., 2020. Disinfection technology of hospital wastes and wastewater: suggestions for disinfection strategy during coronavirus disease 2019 (COVID-19) pandemic in China. Environ. Pollut. 262, 114665. https://doi.org/10.1016/j.envpol.2020.114665.

World Health Organization (WHO), .. . (n.d.). Retrieved from https://covid19.who.int/.

Wright, E.J., Brew, B.J., Wesselingh, S.L., 2008. Pathogenesis and diagnosis of viral infections of the nervous system. Neurol. Clin. 26 (3), 617–633. https://doi.org/10.1016/j.ncl.2008.03.006.

Xiao, F., Sun, J., Xu, Y., Li, F., Huang, X., Li, H., Zhao, J., 2020. Infectious SARS-CoV-2 in feces of patient with severe COVID-19. Emerg. Infect. Dis. 26 (8), 1920–1922. https://doi.org/10.3201/eid2608.200681.

Zamorano Cuervo, N., Grandvaux, N., 2020. ACE2: evidence of role as entry receptor for SARS-CoV-2 and implications in comorbidities. elife 9. https://doi.org/10.7554/eLife.61390.

Zand, A.D., Heir, A.V., 2020. Emerging challenges in urban waste management in Tehran, Iran during the COVID-19 pandemic. Resour. Conserv. Recycl. 162, 105051. https://doi.org/10.1016/j.resconrec.2020.105051.

Zupin, L., Pascolo, L., Zito, G., Ricci, G., Crovella, S., 2020. SARS-CoV-2 and the next generations: which impact on reproductive tissues? J. Assist. Reprod. Genet. https://doi.org/10.1007/s10815-020-01917-0.